arXiv:hep-ph/9903377v1 17 Mar 1999

Photon Plus Jet Production in Large-Q^2 ep Collisions at Next-to-Leading Order QCD

A. Gehrmann-De Ridder[1], G. Kramer[2] and H. Spiesberger[3]

[1] Institut für Theoretische Teilchenphysik, Universität Karlsruhe,
D-76128 Karlsruhe, Germany

[2] II. Institut für Theoretische Physik,* Universität Hamburg,
Luruper Chaussee 149, D-22761 Hamburg, Germany

[3] Institut für Physik, Johannes-Gutenberg-Universität,
Staudinger Weg 7, D-55099 Mainz, Germany

e-mail: gehra@particle.physik.uni-karlsruhe.de,
kramer@mail.desy.de, hspiesb@thep.physik.uni-mainz.de

Abstract

The production of photons accompanied by jets in large-Q^2 deep inelastic ep scattering is calculated in next-to-leading order. We describe how to consistently include contributions from quark-to-photon fragmentation and give numerical results relevant for HERA experiments.

1 Introduction

The production of isolated photons in high-energy hadronic collisions is an important testing ground for QCD. Since the photon does not take part in the strong interaction, it is a "direct" probe of the hard scattering process and provides a means to measure the strong

coupling constant α_s or to extract information on the parton distributions, in particular the gluon density in the proton [1]. Moreover, good knowledge of the standard model predictions for direct photon production is required since it is an important background for many searches of new physics.

At HERA, with increasing luminosity, the measurement of isolated photon production will give information on the parton content of the proton and at $Q^2 = 0$, i.e. for photoproduction, also on the parton distributions in the photon. First experimental results from the ZEUS collaboration [2, 3] (see also [4]) have been reported and found in reasonable agreement with next-to-leading order (NLO) predictions [5]. Cross sections for the production of hard photons in deep inelastic scattering are much smaller as compared to photoproduction and, therefore, more difficult to measure. Typical cross sections, for example with $Q^2 > 10\ GeV^2$, are of the order of 10 pb. With a luminosity of 50 pb^{-1} one thus expects measurements of differential cross sections to become feasible.

A NLO calculation for direct photon production in deep inelastic ep scattering, $ep \rightarrow e\gamma X$, at large Q^2 has been reported recently by two of us and D. Michelsen [6]. Since hard photon production occurs, compared to inclusive deep inelastic scattering, at a relative order O(α) one expects a sizable cross section only at moderately large Q^2. Therefore, one can restrict the calculation to pure virtual photon exchange with Z exchange neglected. In [6] the hadronic final state is separated into $\gamma + (1 + 1)$- and $\gamma + (2 + 1)$-jet topologies (the remnant jet being counted as "+1" jet us usual). The approach is thus analogous to the calculation of $(2 + 1)$- and $(3 + 1)$-jet cross sections, where one of the final state gluons is replaced by a photon [7]. In addition to the direct production, photons can also be produced through the fragmentation of a hadronic jet into a single photon carrying a large fraction of the jet energy [8]. This long-distance process is described in terms of the quark-to-photon and gluon-to-photon fragmentation functions which absorb collinear singularities present in the perturbative calculation. First measurements of the $q \rightarrow \gamma$ fragmentation function in $e^+e^- \rightarrow \gamma + 1$-jet are presented in [9] (see also [10] for the discussion of an inclusive measurement). The NLO theory for this process has been worked out in [11]. In [6] the fragmentation contributions were discarded and the photon-quark collinear singularities had been removed by explicit parton-level cutoffs. The results depended strongly on these photon-parton cutoffs, in particular for the incoming gluon contributions [6]. However, these cutoffs are difficult to control experimentally.

In this paper we report results in which the fragmentation contributions are included together with isolation criteria that limit the hadronic energy in the jet containing the photon. Whereas in [6] various photon + jet cross sections with invariant mass jet resolution criteria were calculated, in this work we concentrate on the calculation of various differential cross sections either exclusively or inclusively which depend on the transverse momenta and rapidities of the photon or the accompanying jet. We use the γ^*p center-of-mass system to define the kinematic variables. The cone method is applied to define the parton jets and to isolate the photon signal.

In section 2 a brief outline of the theoretical background for calculating the cross section

is given. In section 3 numerical results are presented. Section 4 contains a short summary and the conclusions.

2 Subprocesses Through Next-to-Leading Order

2.1 Leading-Order Contributions

In leading order, the production of photons in deep inelastic electron (positron) scattering is described by the quark (antiquark) subprocess

$$e(p_1) + q(p_3) \rightarrow e(p_2) + q(p_4) + \gamma(p_5) \tag{1}$$

where the particle momenta are given in parentheses. The momentum of the incoming quark is a fraction ξ of the proton momentum p_P, $p_3 = \xi p_P$. The proton remnant r has the momentum $p_r = (1 - \xi)p_P$. It hadronizes into the remnant jet so that the process (1) gives rise to $\gamma + (1 + 1)$-jet final states. In the virtual photon γ^*-proton center-of-mass system the hard photon recoils against the hard jet back-to-back. To remove photon production by incoming photons γ^* with small virtuality (photoproduction channel) and to restrict to the case where the scattered electron $e(p_2)$ is observed, one applies cuts on the usual deep inelastic scattering variables x, y and Q^2. In addition, to have photons $\gamma(p_5)$ of sufficient energy we require an explicit cut on the invariant mass W of the final state, $W^2 = (q + p_P)^2$, where q is the electron momentum transfer, $q = p_1 - p_2$ and $Q^2 = -q^2$ as usual. Both leptons and quarks emit photons. The subset of diagrams where the photon is emitted from the initial or final state lepton (leptonic radiation) is explicitly gauge invariant and can be considered separately. Similarly, the diagrams with a photon emitted from quark lines is called quarkonic radiation. In addition, there are also contributions from the interference of these two. Since we are interested in testing QCD under the circumstances that the photon is emitted from quarks the contributions from leptonic radiation are viewed as a background and must be suppressed. This can easily be done by a cut on the photon emission angle with respect to the incoming electron [6]. In our numerical evaluation we include this background source as well as the interference contribution.

At lowest order, each parton is identified with a jet and the photon is automatically isolated from the quark jet by requiring a non-zero transverse momentum of the photon or jet in the γ^*-proton center-of-mass frame. Therefore the photon fragmentation contribution is absent at this order.

2.2 Next-To-Leading Order Corrections

At NLO, processes with an additional gluon, either in the final state or in the initial state, must be taken into account, i.e.

$$e(p_1) + q(p_3) \rightarrow e(p_2) + q(p_4) + \gamma(p_5) + g(p_6), \tag{2}$$

$$e(p_1) + g(p_3) \rightarrow e(p_2) + q(p_4) + \gamma(p_5) + \bar{q}(p_6), \tag{3}$$

where the momenta of the particles are again given in parentheses. In addition, virtual corrections (one-loop diagrams at $O(\alpha_s)$) to the LO process (1) have to be included. The complete matrix elements for (2) and (3) are given in [12]. The processes (2) and (3) contribute both to the $\gamma + (1+1)$-jets cross section, as well as to the cross section for $\gamma + (2+1)$-jets. In the latter case each parton in the final state of (2) and (3) builds a jet on its own, whereas for $\gamma + (1+1)$-jets a pair of final state partons is experimentally unresolved. The exact criteria for combining two partons into one jet will be introduced when we present our results. Following the customary experimental procedure the resolution constraints will be based on the cone algorithm.

In the calculation of the cross section for $\gamma + (1+1)$-jets we encounter the well-known infrared and collinear singularities. They appear for the processes (2) and (3) in those phase space regions where two partons are degenerate to one parton, i.e. when one of the partons becomes soft or two partons become collinear to each other. The singularities are assigned either to the initial state (ISR) or to the final state (FSR). Contributions involving the product of an ISR and a FSR factor are separated by partial fractioning. The FSR singularities cancel against singularities from the virtual corrections to the LO process (1). For the ISR singularities, this cancellation is incomplete and the remaining singular contributions have to be factorized and absorbed into the renormalized parton distribution functions (PDF's) of the proton.

To accomplish this procedure, the singularities are isolated in an analytic calculation with the help of dimensional regularization. This is difficult for the complete cross sections of the processes (2) and (3). After partial fractioning, the phase-space slicing method [13] is used to separate the singular regions in the 4-particle phase space and to determine in these regions the approximated matrix elements and phase space factors. In those regions only, the calculation is performed analytically. For this purpose a slicing cut y_0^J is applied to the scaled invariant masses y_{ij}, where $y_{ij} = (p_i+p_j)^2/W^2$ with $W^2 = (p_P+p_1-p_2-p_5)^2$. y_0^J must be chosen small enough, so that terms of the order $O(y_0^J)$, which are discarded due to the singular approximation, are so small that an accuracy of a few percent can be achieved for the final result.

To be somewhat more explicit, let us assume that by partial fractioning the contribution proportional to the pole term $1/y_{46}$ has been isolated in the matrix element $|M|^2$ for the process (2). In the infrared region $p_6 \rightarrow 0$ the two invariants y_{46} and y_{36} vanish. Then the integration over these two variables is performed: (i) over the singular region (S), $y_{46} < y_0^J$, $y_{36} > 0$, analytically with $4 - 2\epsilon$ dimensions and using the singular approximation; (ii) over the finite region (F), $y_{46} > y_0^J$, $y_{36} < y_0^J$, numerically without any approximation to $|M|^2$ and in 4 dimensions; and (iii) over the explicit two-parton region (R), $y_{46} > y_0^J$, $y_{36} > y_0^J$, also numerically. This separation yields two contributions, the parton-level

4

$\gamma + (1 + 1)$-jets, which come from the integration over the regions (S) and (F) and the parton-level $\gamma + (2 + 1)$-jets contribution, which corresponds to the integration over the region (R). All the remaining phase space integrations are performed numerically with usual Monte Carlo routines. For the physical cross sections defined in the next section, which are obtained by adding the contributions from the regions S, F and R, of course, and after adding the virtual contributions and performing the subtraction of the remaining ISR collinear singularities, the dependence on the slicing parameter y_0^J cancels. This has been checked in [6]. This means that the cut-off y_0^J is purely technical.

In addition, the matrix elements $|M|^2$ for the processes (2) and (3) have *photonic* infrared and collinear singularities, i.e. due to soft or collinear photons. The infrared singularity can not occur since we require a sufficiently large photon energy $E_\gamma = |\vec{p_5}|$. But collinear singularities are present in general. In the earlier work [6] these q-γ collinear contributions were eliminated by an isolation cut on the photon of the form $y_{5i} > y_0^\gamma$ with a sufficiently large isolation parameter y_0^γ which was considered as a physical cut. In this approach, the photon was considered as a special parton, which was always isolated from all other partons in the initial and final state. Such a photon isolation is very difficult to impose experimentally, since it refers to a separation of the photon from partons, whereas in the experiment only hadrons are measured directly which are recombined to jets. In addition, it was found in [6] that the results, in particular for the gluon-initiated process (3), depend strongly on the isolation cut y_0^γ. In (3) the photon can become collinear to two final state partons, namely q and $\bar{q}$, which explains the stronger dependence compared to the process (2), where there is only one quark (or antiquark) in the final state. Although under the kinematical conditions assumed in [6] the contribution of the process (3) was only some fraction of the total cross section for $\gamma + (1 + 1)$-jets, the y_0^γ dependence of the final result was undesirable. In a more systematic treatment the y_0^γ dependence can be avoided by adding contributions from the quark-to-photon fragmentation function (FF). In order to achieve this we include the contributions to $|M|^2$ from (2) and (3), where $y_{5i} < y_0^\gamma$ with $i = 4$ in (2) and $i = 4$ and 6 in (3). This leads to collinear divergent contributions which are regulated by dimensional regularization. The divergent part is absorbed into the bare photon FF to yield the renormalized FF denoted by $D_{q \to \gamma}$. The additional fragmentation contribution, which includes the contributions from the region $y_{5i} < y_0^\gamma$ $(i = 3, 4)$, has, for example, for the process (2) the following form

$$| M |^2_{\gamma^* q \to qg\gamma} = | M |^2_{\gamma^* q \to qg} \otimes D_{q \to \gamma}(z) \tag{4}$$

where $D_{q \to \gamma}(z)$ in (4) is given by [14]

$$D_{q \to \gamma}(z) = D_{q \to \gamma}(z, \mu_F^2) + \frac{\alpha e_q^2}{2\pi} \left(P_{q\gamma}(z) \ln \frac{z(1-z) y_0^\gamma W^2}{\mu_F^2} + z \right). \tag{5}$$

$P_{q\gamma}(z)$ is the LO quark-to-photon splitting function

$$P_{q\gamma}(z) = \frac{1 + (1 - z)^2}{z} \tag{6}$$

5

and e_q is the electric quark charge. $D_{q \to \gamma}(z, \mu_F^2)$ stands for the non-perturbative FF of the transition $q \to \gamma$ at the factorization scale μ_F. This function will be specified in the next section when we present our results. The second term in (5), if substituted in (4), is the finite part of the result of the integration over the collinear region $y_{5i} < y_0^\gamma$. As will be explicitly shown in [15], the y_0^γ dependence in (5) cancels the dependence of the numerically evaluated $\gamma + (1 + 1)$-jet cross section restricted to the region $y_{5i} > y_0^\gamma$, investigated in [6]. The variable z stands for the fraction of the photon energy in terms of the energy of the quark that emits the photon. Suppose the photon is emitted from the final state quark with 4-momentum $p_4' = p_4 + p_5$, then z can be related to the invariants y_{35} and y_{34}

$$z = \frac{y_{35}}{y_{34'}} = \frac{y_{35}}{y_{34} + y_{35}} \tag{7}$$

The fragmentation contribution is proportional to the cross section for $\gamma^* q \to qg$, which is of $O(\alpha_s)$ and well known. It must be convoluted with the function in (5) as indicated in (4) to obtain the contribution to the cross section for $\gamma^* q \to qg\gamma$ at $O(\alpha\alpha_s)$. Equivalent formulas are used to calculate the fragmentation contributions to the channel (3) and in the case where the quark in the initial and final state is replaced by an antiquark in (2).

3   Results

The results presented in this section are obtained for energies and kinematical cuts appropriate for the HERA experiments. The energies of the incoming electron (positron) and proton are $E_e = 27.5 \ GeV$ and $E_P = 820 \ GeV$, respectively. The cuts on the usual DIS variables are

$$Q^2 \geq 10 \ GeV^2, \qquad W > 10 \ GeV, \tag{8}$$
$$10^{-4} \leq x \leq 0.5, \qquad 0.05 \leq y \leq 0.95.$$

To eliminate the background from lepton radiation [6] we require

$$90° < \theta_\gamma < 173°, \quad \theta_{\gamma e} \geq 10° \tag{9}$$

where θ_γ is the emission angle of the photon measured with respect to the momentum of the incoming electron in the HERA laboratory frame. The cut on $\theta_{\gamma e} = \sphericalangle (e(p_2), \gamma(p_5))$ suppresses leptonic radiation from the final-state electron. The PDF's of the proton are taken from [16] (MRST) and α_s is calculated from the two-loop formula with the same Λ value ($\Lambda_{\overline{MS}}(n_f = 4) = 300 \ MeV$) as used in the MRST parametrization of the proton PDF. The scale in α_s and the fractorization scale are equal and fixed to Q^2.

We are interested in the differential two-particle inclusive cross section $E_\gamma E_J d\sigma / d^3 p_\gamma d^3 p_J$ at NLO (up to $O(\alpha\alpha_s)$), where $(E, \vec{p})$ represents the four-vector momentum of the γ or jet. The $\gamma + (1 + 1)$-jet cross section receives contributions from leading and next-to-leading order and the $\gamma + (2 + 1)$-jet cross section from leading order only. In the latter case, only

$\gamma + 2$-parton-level jets contribute, while each parton including the photon build a jet on their own. The evaluation of the $\gamma + (1+1)$-jet cross section is based on two separate contributions, a set of two-body contributions, i.e. $\gamma + 1$ parton-level jet, and a set of three-body contributions, i.e. $\gamma + 2$ parton-level jets. In this definition of parton-level jets the remnant jet " $+ 1$" is not counted whereas the photon is considered also as a parton, like $q, \bar{q}$ and g. Each set of contributions is completely finite as all infrared and collinear singularities have been canceled or absorbed into the proton PDF or the quark-to-photon FF. Each contribution to the $\gamma + (1+1)$-jet cross section depends separately on the slicing parameter y_0^J. The analytic contributions are valid only for very small y_0^J. Separately, the two contributions have no physical meaning. For the contributions to the $\gamma + (1+1)$-jet cross section coming from $\gamma + 2$ parton-level jets, a slicing cut y_0^γ for the photon is introduced. After adding the photon fragmentation contribution this sample becomes independent of y_0^γ, i.e. also y_0^γ has the status of a technical cut like y_0^J. In the $\gamma + 1$ parton-level jet event sample the photon is isolated from q and $\bar{q}$ by requiring a non-zero transverse momentum of the photon in the $\gamma^* p$ center-of-mass frame. The two technical cuts y_0^J and y_0^γ serve only to distinguish the phase space regions, where the integrations have been done analytically with arbitrary dimensions from those where they have been done numerically in four dimensions. These two parameters must be chosen sufficiently small to justify the neglect of terms proportional to y_0^J and y_0^γ, respectively in the analytical part of the calculations. We found that $y_0^J = 10^{-4}$ and $y_0^\gamma = 10^{-5}$ is sufficient to fulfill this requirement.

In order to comply with the jet definitions in future analyses of experimental measurements the partons and the photon in the $\gamma + 2$ parton-level jet sample are recombined to $\gamma + (1+1)$-jets using the cone algorithm of the Snowmass convention [17]. In this recombination scheme the photon is treated like any other parton (so-called democratic algorithm). In the $\gamma^* p$ center-of-mass frame, two partons i and j are combined into a jet J if they obey the cone constraint $R_{i,J} < R$, where

$$R_{i,J} = \sqrt{(\eta_i - \eta_J)^2 + (\phi_i - \phi_J)^2}. \tag{10}$$

η_J and ϕ_J are the rapidity and azimuthal angle of the recombined jet. These variables are obtained by taking the averages of the corresponding variables of the recombined partons i and j multiplied with their p_T values. The p_T of jet J is the sum of $p_{T,i}$ and $p_{T,j}$. We choose $R = 1$. In some cases, an ambiguity may occur, when two partons i and j qualify both as two individual jets i and j and as a combined jet J. In this case we count only the combined jet J to avoid double counting. The rapidity is always defined positive in the direction of the proton remnant momentum. The azimuthal angle is defined with respect to the scattering plane given by the momentum of the beam and the scattered electron. One of the recombined jets may be the photon jet. To qualify a jet as a photon jet we restrict the hadronic energy in this jet by requiring

$$z_\gamma = \frac{p_{T,\gamma}}{p_{T,\gamma} + p_{T,had}} = 1 - \epsilon_{had} > z_{cut}. \tag{11}$$

$p_{T,\gamma}$ and $p_{T,had}$ denote the transverse momenta of the photon and the parton producing hadrons in this jet, respectively. For our predictions we choose $\epsilon_{had} \leq \epsilon_{had}^0 = 0.1$ [2]. Eventually the parameter ϵ_{had}^0 (or z_{cut}) must be chosen in accordance with the experimental analysis. Our results depend also on the choice of the quark-to-photon fragmentation function. The factorization scale dependent quark-to-photon FF of $O(\alpha)$ is taken from [14]. It is the sum of two contributions, the solution of the evolution equation at this order and an initial FF at some initial scale μ_0. The initial FF function and initial scale have been fitted to the ALEPH $\gamma + 1$-jet data [9]. The factorization scale dependent quark-to-photon fragmentation function also gives a good description of the inclusive photon distribution as measured by OPAL [10].

With these definitions it is clear that in NLO the final state may consist of two or three jets, where one jet is always a photon jet. The three-jet sample, equivalent to $\gamma + (2+1)$-jets in the notation of the previous sections, consists of all $\gamma + (2+1)$ parton level jets, which do not fulfill the cone constraint (10).
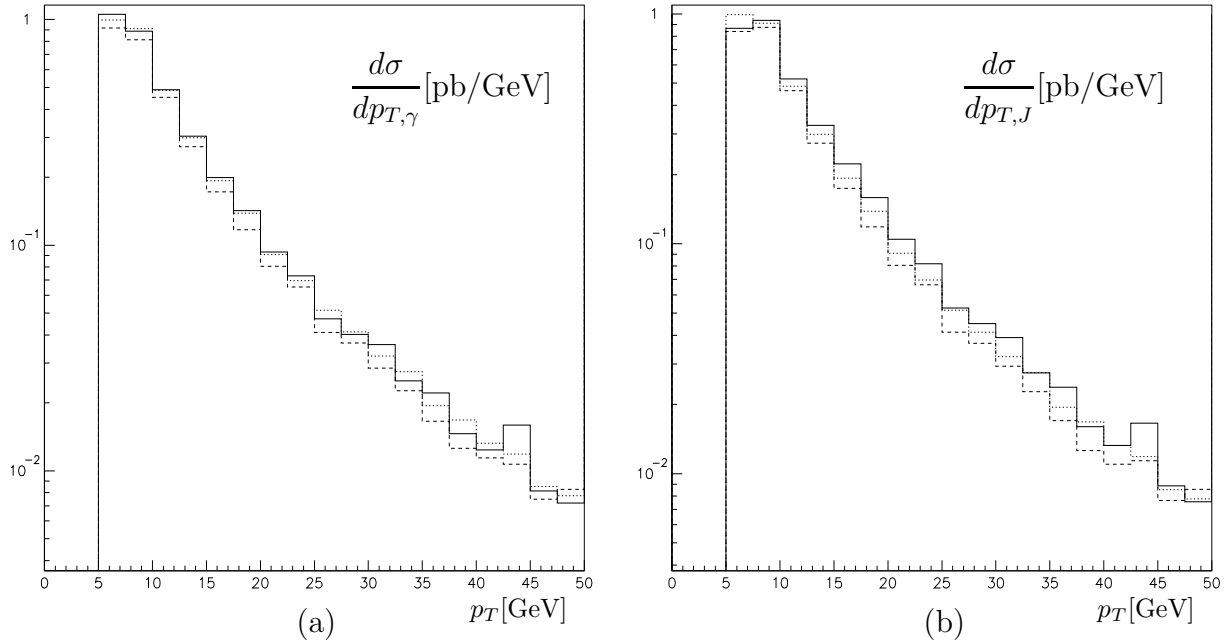

Figure 1: p_T distributions of photon (a) and jet with largest p_T (b) for LO (dotted line), NLO $\gamma + (1+1)$-jets (dashed line) and NLO $\gamma + (1+1)$- and $\gamma + (2+1)$-jets (full line).

In Fig. 1 and 2 we show our results for the p_T and η dependence of the cross sections, $d\sigma/dp_T$ and $d\sigma/d\eta$, concerning the photon and the jet with the largest p_T. In each figure we have plotted three curves, (i) the cross section in LO (dotted curve), which has only $\gamma + (1+1)$-jets and is independent of the jet defining parameters R and ϵ_{had}^0, (ii) the NLO cross section for $\gamma + (1+1)$-jets (dashed curve) and (iii) the sum of the NLO cross sections for $\gamma + (1+1)$-jets and $\gamma + (2+1)$-jets (full curve). Specifically, in Fig. 1a we present $d\sigma/dp_{T,\gamma}$, the transverse momentum dependence of the three cross sections (i),
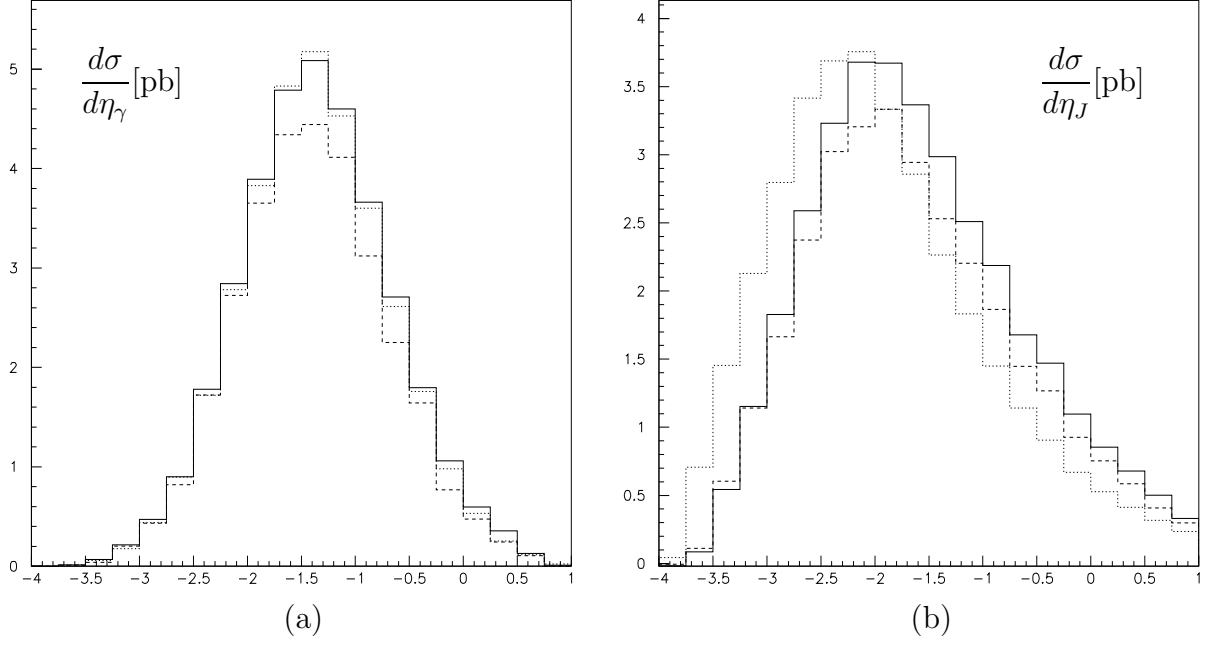
Figure 2: η distributions of photon (a) and jet with largest p_T (b) with labeling of curves as in Fig. 1.

(ii) and (iii) for $p_{T,\gamma} \geq 5 \ GeV$. All other variables, in particular η_J, η_γ and $p_{T,J}$, are integrated over the kinematically allowed ranges. We see that all three cross section have a similar shape. The sum of the $\gamma + (1+1)$- and $\gamma + (2+1)$-jets cross section is only slightly larger than the $\gamma + (1+1)$-jets cross section. Both cross sections do not differ very much from the LO cross section indicating that the NLO corrections are not very large. Of course, this is a consequence of our choice for the cone radius R. In Fig. 1b the plot of $d\sigma/dp_{T,J}$ for the jet with the largest p_T is shown. The qualitative behaviour of the three cross sections (i) - (iii) is similar as in Fig. 1a. For the η distributions we integrate over $p_{T,\gamma} \geq 5 \ GeV$ and $p_{T,J} \geq 6 \ GeV$. The choice of two different values of minimal p_T's for the photon and the jet is necessary to avoid the otherwise present infrared sensitivity of the NLO predictions. This sensitivity is known from similar calculations of dijet cross sections in ep collisions [18] and must be avoided. The cross section $d\sigma/d\eta_\gamma$ is plotted in Fig. 2a, again for the three cases (i), (ii) and (iii). The shapes of the three curves are similar. Here we have integrated over the full kinematic range of the variable η_J. Figure 2b contains the predictions for $d\sigma/d\eta_J$, where η_J is the rapidity of the jet with the largest p_T. In Fig. 2b we observe that the full curve, which represents $d\sigma/d\eta_J$ for the sum of the two jet cross sections, is shifted somewhat more to $\eta_J > 0$ compared to the NLO $\gamma + (1+1)$-jets cross section. The LO cross section (dotted curve) peaks more in the backward direction than the other two. Compared to $d\sigma/d\eta_\gamma$, shown in Fig. 2a the η_J distribution for the jet peaks at somewhat smaller η_J.

For completeness we also give the results for the various cross sections in Table 1, separated

9

Table 1: Contributions to the cross sections (in pb) for $\gamma + (1+1)$- and $\gamma + (2+1)$-jet production (see text).

Contribution	$\gamma + (1+1)$-jets	$\gamma + (2+1)$-jets
LO	8.561 ± 0.022	
S	-32.164 ± 0.026	
R$(q, \bar{q})$	24.843 ± 0.034	0.6349 ± 0.0008
R(g)	3.717 ± 0.005	0.3239 ± 0.0007
F	3.429 ± 0.022	
D	-0.599 ± 0.001	
sum	7.787 ± 0.053	0.9588 ± 0.0010

into the contributions S, R (for incoming quarks or antiquarks and incoming gluons), F as described in the previous section and the fragmentation contribution denoted by D as defined in Eq. (5). About $12\,\%$ of the total NLO cross section is due to $\gamma + (2+1)$-jet final states. The $\gamma + (1+1)$-jets cross section is reduced by about $9\,\%$ by NLO corrections.

4   Concluding Remarks

We have presented a NLO calculation for the production of photons accompanied by jets in deep inelastic electron proton scattering, taking into account the contribution from quark-to-photon fragmentation. This improves a previous work which suffered from the presence of parton-level cutoff parameters. The present consistent treatment allows for a direct comparison of our theoretical predictions with experimental measurements without being sensitive to uncertainties from unphysical cutoff parameters.

We expect that the measurement of photon plus jet production at HERA will contribute to testing perturbative QCD. Moreover, our results add another piece to the set of NLO predictions of the standard model needed in searches for new physics. The calculation covers the range of large Q^2 up to several $10^3 \ GeV^2$. At even larger momentum transfers additional contributions from Z exchange become as important as pure γ exchange to which the present work was restricted.

References

[1] A. D. Martin, R. G. Roberts and W. J. Stirling, Phys. Lett. B387 (1996) 419

[2] J. Breitweg et al., ZEUS Collaboration, Phys. Lett. B413 (1997) 201

[3] ZEUS Collaboration, submitted to *ICHEP XXIX*, Vancouver, 1998, Abstract 815; P. J. Bussey, Proc. *Workshop on Photon Interactions and the Photon Structure*, Lund, Sweden, 10 - 13 Sep 1998

[4] H1 Collaboration, submitted to *HEP 97*, Jerusalem, 1997, Abstract 265

[5] L. E. Gordon, Phys. Rev. D57 (1998) 235

[6] G. Kramer, D. Michelsen and H. Spiesberger, Eur. Phys. J. C5 (1998) 293

[7] D. Graudenz, Phys. Lett. B256 (1991) 518, Phys. Rev. D49 (1994) 3219; T. Brodkorb and E. Mirkes, Z. Phys. C66 (1996) 141; E. Mirkes and D. Zeppenfeld, Phys. Lett. B380 (1996) 205

[8] K. Koller, T. F. Walsh and P. M. Zerwas, Z. Phys. C2 (1979) 197; E. Laermann, T. F. Walsh. I. Schmitt and P. M. Zerwas, Nucl. Phys. B207 (1982) 205

[9] D. Buskulic et al., ALEPH Collaboration, Z. Phys. C69 (1996) 365

[10] K. Ackerstaff et al., OPAL Collaboration, Eur. Phys. J. C2 (1998) 39

[11] A. Gehrmann-De Ridder, T. Gehrmann and E. W. N. Glover, Phys. Lett. B414 (9197) 354; A. Gehrmann-De Ridder and E. W. N. Glover, Nucl. Phys. B517 (1998) 269

[12] D. Michelsen, doctoral thesis, University of Hamburg, 1995, DESY 95-146

[13] K. Fabricius, G. Kramer, G. Schierholz and I. Schmitt, Z. Phys. C11 (1982) 315; F. Gutbrod, G. Kramer and G. Schierholz, Z. Phys. C21 (1984) 235; W. T. Giele and E. W. N. Glover, Phys. Rev. D46 (1992) 1980

[14] E. W. N. Glover and A. G. Morgan, Z. Phys. C62 (1994) 311; A. Gehrmann-De Ridder and E. W. N. Glover, Eur. Phys. J. C7 (1999) 29

[15] A. Gehrmann-De Ridder, G. Kramer and H. Spiesberger, (in preparation)

[16] A. D. Martin, R. G. Roberts, W. J. Stirling and R. S. Thorne, Eur. Phys. J. C4 (1998) 463

[17] J. E. Huth et al., Proc. *Summer Study on High Energy Physics, Research Directions for the Decade*, Snowmass, 1990; F. Abe et al., CDF Collaboration, Phys. Rev. D45 (1992) 1448; M. Seymour, Z. Phys. C62 (1994) 127

[18] G. Kramer and B. Pötter, Eur. Phys. J. C5 (1998) 665